CBM 015

STUDIES OF FRACTURE MECHANICS OF COAL

FINAL TECHNICAL REPORT

FOR THE PERIOD

1 JUNE 1979 - 30 NOVEMBER 1980

WILLIAM R. POWELL

MECHANICAL ENGINEERING & MECHANICS
COLLEGE OF ENGINEERING
WEST VIRGINIA UNIVERSITY
MORGANTOWN, WV 26506

PREPARED FOR THE
U.S. DEPARTMENT OF ENERGY
UNCONVENTIONAL GAS RECOVERY PROGRAM
MORGANTOWN ENERGY TECHNOLOGY CENTER
UNDER CONTRACT DE-AT-21-79MC11284, TASK ORDER #2.

CONTENTS

Executive Summary ii

I. Introduction 1

II. Purpose. 3

III. Literature Review 6

IV. Results 31

V. Conclusions 83

VI. Recommendations 88

VII. References 91

VIII. Appendices 102

1. Experimental Equipment 103
2. Experimental Proceedures 117
3. Specimen Procurement, Storage and Preparation . 131
4. Fracture Toughness Test Results, Coal. 136
5. Hydraulic Fracture Results for Coal 149
6. Model Equations for Anisotropic Material 156
7. Fracture Toughness Test Results, Limestone and Sandstone 166
8. Finite Difference Analysis 170

Executive Summary

The purpose of the research project was to gain more knowledge of the basic fracture mechanics behavior of coal and of its response to hydraulic fracturing. The work concentrated on experimental measurements; theoretical explanations and analytical modeling were secondary.

Eighty successful fracture toughness tests were performed on notched beam specimens (using modified ASTM E-399 Standard Test Method). The results indicate that the critical stress intensity factor (K_{Ic}) for coal is approximately 50-100 psi-$\sqrt{in}$(compared to 1000 psi-$\sqrt{in}$ for limestone and 40,000 psi-$\sqrt{in}$ for high strength steels). There are significant variations in K_{Ic} between coal seams and also with testing orientation within one coal seam. These are explained by measured variations in the ultimate tensile strength of the coal. For coal, like for other rocks, the fracture toughness is determined by tensile strength rather than by strain energy.

Thirty eight hydraulic fracture simulations were performed. They showed that coal behaved as predicted by a published theoretical model for hydraulic fracturing of isotropic materials. However, the fracture pressure and tensile strength were found to be rate dependent. Also, the tensile strength for hydraulic fracturing was calculated to be a factor of ten larger than measured in tensile testing. This unexpected result is tentatively attributed to size effects in the specimens.

Except for questions of rate and size effects, enough information was obtained to be able to develop computer models to predict underground hydraulic fracture behavior of coal. More testing similar to previous tests should be able to quantify the size and rate effect so numerical results of laboratory simulations could be scaled up to field test situations.

I. INTRODUCTION

Methane gas, a natural byproduct of the chemical reactions that produce coal, is trapped in varying amounts in coal seams. The amount of methane depends on the petrography of the coal seam, the depth (confining stresses) and the properties of the adjacent rock layers. With a heat content of 900 Btu/SCF, methane represents a potentially valuable fuel source if it can be recovered from the coal. Because of the permeability characteristics of coal, methane flow rates from vertical wells drilled into coal seams decrease quickly.

When applied to coal beds for methane drainage, the traditional methods of stimulating gas and oil reservoirs have failed to produce gas flow rates large enough to economically justify developing this resource. The major problem is recognized (1) to be that coal has very low permeability with gas flow occurring only through fractures. Stimulating production by hydraulic fracturing is the most promising stimulation technique but it is often not able to produce the gas quantities necessary for economic viability. Fracturing is an uncertain technique because of the inability to predict the direction, shape, or lateral extent of the fractures. Knowledge of the fracture pattern is critical in methane drainage to evaluate the possibility that the fractures will penetrate the roof rock and jeopardize its structural integrity during subsequent mining operations.

To improve fracturing techniques, more fundamental knowledge of the mechanisms controlling fracture initiation and growth in coal is needed. This knowledge will lead to improved predictions, and perhaps control, of fracture patterns developed and understanding of when fractures will cross stratigraphic sections such as bedding planes, fault cleats

and other fractures. Research in this area has provided either qualitative results (1) or largely theoretical analyses (2,3). First the real mechanisms and physics of fracturing need to be identified in a quantitative manner and, then, empirical or theoretical elastic models need to be developed to describe fracturing in cleated coalbeds. Time and sequence dependence of the fracturing process have not been investigated theoretically and may explain or improve the success of fracturing techniques such as the Kiel process.

II. PURPOSE

This project was completed in a series of individual tasks involving basic research including the development of models on the mechanical behavior of coal which can be used to predict fracture patterns in the field and the interpretation of data from field tests in terms of the models developed.

2.1 Quantification of Fracture Properties

a. Task 1 - Quantifying the Fracture Toughness of Coal

Experimental tests using a modification of the ASTM E399-74 procedure were performed on coal samples. These tests were originally conducted to determine fracture toughness of coal for finite element analyses of the stresses around coal mines. This task was a continuation of ongoing research but concentrated on the materials relevant to gas recovery from gassy coalbeds. The loading rates of these were varied to study time-dependent behavior. The coal specimens were also analyzed for moisture content and ash content.

b. Task 2 - Identifying Directions of Natural Weakness in These Materials (e.g., Butt Cleats, Face Cleats) and Determining Their Relative Strengths

Experiments like those in Task 1 were performed on specimens cut at different orientations to the geological strata. Coal specimen faces initially tested were orthogonal to the bedding plane, butt and face cleats. Specimens tilted relative to these planes were next tested to detect directions the fractures take.

c. Task 3 - Experimentally Measuring the Interactions of Stresses, Directions of Weakness and Fracture Orientation

Facilities and procedures similar to those used by Hanson, et al., (4), were developed to produce fractures by pressurizing holes in cubes of material. Uni-, bi- and triaxial compressive loads were applied before fracture. Fracture pressures and directions were recorded. The holes were drilled at different orientations relative to the strata. Pressurization was produced by pumping fluid into the holes.

d. Task 4 - Determining the Influence of Liquid Flow Rates, Viscosity and Simulated Tectonic Stresses on the Propagation of Hydraulically Induced Fractures.

Experiments like those in Task 3 were conducted using only one orientation of the material but using fluids of different viscosities and different secondary confining stresses. The amount of fluid entering the hole was measured as was the rate of fracture growth. Different confining stresses were used and relations between stress, flow rate and permeability were examined.

e. Task 5 - Developing Models for the Mechanical Behavior of Coal Which Can be Used to Predict Fracture Patterns in the Field.

Models were developed which describe coal more accurately than isotropic elastic models. This task involved review of the data from Tasks 1, 2 and 3 and selecting the most appropriate model. The model selected is an orthotropic material with fracture toughness governed by a maximum stress criterion.

f. Task 6 - Experimentally Examining the Ability, Under Various Stress States, of Cracks in These Materials To Propagate Across Joints, Other Fractures and Across Boundaries into Surrounding Rocks.

This task involved tests such as those in Task 1 with specimens containing both coal and adjacent material. Those materials, stresses and orientations for which cracks propagate across the boundary were to be identified. Again, orientations for which fractures cross the existing crack were identified.

2.2 Supplemental Project

a. Task 7 - Comparison of Fracture Properties of Coal With Those of the More Thoroughly Studied Limestone and Berea Sandstone.

Tests similar to those of Tasks 1 and 3 were performed on specimens of sandstone and limestone. These results were used in analyses predicting fracture propagation from coal into neighboring strata.

III. LITERATURE REVIEW

This literature review will focus on topics related to the mechanical properties of coal, mechanics of fracture in rocks and their consequent use in the study of hydraulic fracturing phenomenon. This chapter will be divided into the following sections:

1. Theory of fracture mechanics in brittle materials
2. Fracture toughness determination of rocks and other standard materials.
3. Mechanical properties of coal.
4. Hydraulic fracturing experiments - field and laboratory.
5. Fluid flow problem in hydraulic fracturing - numerical approach to single phase and two phase flow through porous permeable media.
6. Analysis of hydraulic fracturing - determination of fracture dimension, fracture penetration, etc., by means of different numerical methods.

This review will attempt to project an overview of the related analytical and experimental description of hydraulic fracturing that has been undertaken in the recent past. Identification of such theories and descriptions will be useful in the development of fracture models of coal and their subsequent use in hydro-fracturing processes.

3.1 Theory of Fracture Mechanics in Brittle Material

The first analytical model of fracture mechanics was put forth by Griffith (5). Griffith evaluated the decrease of strain-energy when cracks (length 2a) were formed and equated it to the energy required to form new crack surfaces. Thus the concept of fracture toughness of material was generated.

When the load or crack size is kept below a threshold value of unstable crack extension, the magnitude of the stress field around a sharp crack is measured by the so called "stress-intensity-factor" (K). The factor K is a measure of the amplitude of the stress field covering the region surrounding the crack tip. The quantity K_c (fracture toughness) is interpreted as the maximum value of K (stress intensity factor) beyond which the crack becomes unstable.

For biaxial or triaxial state of stress, around a crack tip, the expression for stress-field in terms of single parameter K becomes inadequate. Here three parameters, K_I (plane-symmetric loading), K_{II} (skew-symmetric loading) and K_{III} (antiplane shear), describing three different modes of crack deformations are needed. Irwin (6) observed that there were three independent kinematic movements (modes I, II & III) of the upper and lower crack surfaces to each other, which could be related to these three parameters. They are necessary and sufficient to describe all possible modes of crack behavior in the most general state of elastic stress.

Several mixed mode fracture criteria are available in the literature. All these theories assume isotropy and linear elastic

behavior. These criteria are as follows:

(a) Maximum tensile hoop stress theory (7)

(b) Minimum strain energy density theory (3),

(c) Maximum strain energy release rate (8),

(d) Crack closure and frictional effects theory (9).

The first three theories have been discussed and compared by Ingraffea (10).

Since the stress-field equations indicate that the stress becomes infinite as we approach the crack-tip, formation of a plastic zone around the crack tip is postulated to account for finite stress. By using von-Mises yield criterion, an approximation of the size of the plastic zone was made by McClintock and Irwin (11).

The apparent fracture toughness of rock was shown to be dependent on crack length by Ingraffea and Schmidt (12), similar to metallic materials. However, unlike metals, Schmidt and Lutz (13) showed that the thickness of the specimen had no effect on toughness. With the help of these findings, Schmidt (14) postulated that a crack tip process zone existed for rock but was different from the plastic zone in metals. The inelastic behavior in a rock at the crack tip was described as microcracking by Hardy (15). This gave rise to the maximum normal stress criterion where the von-Mises yield condition was replaced by the criterion of maximum normal tensile stress.

Evaluation of the stress field around a crack tip, and determination of expressions for stress intensity factor for different

crack geometries and loading conditions have been reported in numerous papers. Sack (16) discussed the three dimensional aspects of the Griffith theory of brittle fracture by taking a circular crack as a degenerate case of an oblate spheroid. Sneddon (17) applied the Hankel transform and obtained stresses near circular crack. The penny-shaped crack has been studied by Keer (18), Payne (19), Green and Zerna (20), Collins (21) and others. In the previous six references, the crack is opened by load applied symmetrically with respect to crack faces. Westmann (22) solved the asymmetric mixed boundary-value problem.

Irwin (23) derived the stress intensity factor in mode I, by assuming the crack shape to be elliptical and using the solution to the problem of a flat elliptical crack as obtained by Green and Sneddon (24). Sadowsky and Sternberg (25) considered the stress concentration around a triaxial ellipsoidal cavity in a body of infinite dimensions. In the case of the elliptical crack, although the expression for K_1 (stress intensity factor in mode I) is relatively simple, the expressions for K_2 and K_3 become functions of material constants and elliptic functions related to the geometry and dimension of the crack. Kassir and Sih (26) derived expressions for stress intensity factors under arbitrary loading. Shah and Kobayashi (27) formulated the stress intensity factor of an elliptic crack under arbitrary normal loading. Here the internal pressure was assumed to be a polynomial of the x and y coordinates. All the analyses in the previous papers were done for a linear

elastic isotropic and homogeneous body.

The two dimensional elastic problem of crack in a bi-material space has been solved different ways. Erdogan (28) and Williams (29) solved the problem of a crack in the interface of two infinite dissimilar media by using complex variable formulation. England (30) showed that the problem of a single line crack opened by equal and opposite normal pressure between two bonded dissimilar half planes is physically inadmissible. Different solution methods of the integral equations generated by the elasticity equations have been developed (e.g., Erdogan and Gupta (31), Dhawan and Dhaliwal (32), etc.). The problem of a crack parallel to the interface has been solved for different material and loading configurations (e.g., Erdogan and Gupta (33), Rice and Sih (34), Erdogan (35), Calhoun and Lowengrub(36), Atkinson (37), Erdogan and Gupta (38)). Erdogan and Arin (39) considered the problem of a penny shaped crack in two dissimilar media.

The companion problem is that of a crack oriented perpendicular to the interface of two dissimilar media. Cook and Erdogan (40) solved the problem of a crack perpendicular to the interface of two dissimilar half planes. They showed that if the materials [1] and [2] are bonded together with a perfect interface and if $G_1 < G_2$, with the crack in the material [1], then the stress intensity factor approaches zero as the crack approaches the interface. Conversely, if $G_2 < G_1$, the corresponding stress intensity factor approaches infinity. This problem, for various loading and crack locations

has been solved by different investigators (e.g., Atkinson (41), Erdogan and Biricikoglu (42), Gupta (43), Goree (44), Ashbaugh (45)). Rudolphi and Ashbaugh (46) used similar methods to calculate the stress factor of crack approaching the interface of a bounded elastic body.

Although the two dimensional elastic solution predicts that a crack originating in a softer material will not cross a perfect interface bonded to a stiffer material, the experimental evidences show that the crack does cross such interfaces. Anderson (47) showed under laboratory conditions that the cracks did propagate through unbonded interfaces and their frequency of success was a strong function of the applied normal force and induced frictional force. Anderson et al. (48) carried out further investigation by observing the growth of hydraulic fracture near the interface between different media (sandstone, limestone, plexiglass, etc.). Dally and Kobayashi (49), showed through a photo-elastic study that cracks did propagate through an interface joining different kinds of plastics (homelite and epoxy-KTE_2). It was shown that the dynamic effect played a significant role at the interface.

Atkinson (50), considered the transient problem of crack in a media with spatially varying elastic moduli. Steady-state analysis of the crack propagation in such a media was also considered. The crack problem, with two dissimilar media, bonded through a "diffused-interface" was also considered by Atkinson (51). It was shown that, with the assumption of existence of an interface where

the elastic properties change continuously (as opposed to step change in the case of perfect interface), the value of the stress-intensity factor remained non-zero and bounded. Only the antiplane shear (mode III) loading was considered for the problem.

The problem of a crack in a finite anisotropic body with general loading has not been solved analytically. Also problems similar to Atkinson (51), but in mode I, mode II or mixed mode, have not been solved numerically. The complexity of the solution of simpler problems, suggests that the finite-element-method will be the most efficient way of solving such problems.

A singularity element is introduced by most investigators to conduct a viable stress analysis around a crack tip by the finite-element method. Hilton and Sih (52) reported various methods and singularity elements developed. Wilson (53) presented solutions by combining singularity elements and more conventional elements. Tracey (54) investigated the stress field around a crack tip for mode I and mode II, in three dimensions. A program for a singularity finite element is also provided. Development of hybrid elements was discussed by Orringer (55), and Apostal, et al. (56), Atluri, et al. (57). Benzley and Parks (58) gave an excellent review of all the commercially available programs with crack tip singularity elements.

The analytical solution of the problem of a crack in triaxial state of stress is extremely involved, even in an isotropic medium. Creese and Meyers (59) discussed the stress analysis problem in three dimensions. They used a boundary-integral-equation (BIE)

method for a crack in an isotropic and homogeneous medium. The BIE method is used with a normalization procedure for calculating stress intensity factors for various elliptic cracks. Weaver (60) formulated an approach which utilizes a system of integral equations designed over the crack area and solved for the unknown dislocations to yield all other quantities related to the crack and spatial co-ordinates. Derivation of the system of equations, numerical procedures and stress intensity factors for rectangular cracks were reported.

Gross and Strawley (61) calculated the stress-intensity factors for three-point bend specimens. These investigators applied a boundary value collection procedure to the Williams stress function. Thus the values for stress intensity factors were calculated, for simple edge cracks in rectangular section specimens subjected to three-point bending. A similar procedure was applied to determine the values of stress intensity factors for single edge cracks of various depths in specimens subjected to pure bending and combined bending and tension (62). It was shown that the K_{Ic} measurement capacity of such specimens was not very sensitive to the eccentricity of loading. These investigations form the basis of the standard testing procedure for determining fracture toughness in metals.

2.2 Fracture Toughness Determination

The standard method of test for plane-strain fracture toughness of metallic materials was developed by the American Society for Testing and Materials (63). The basis for development of this test method in terms of linear elastic fracture mechanics was formulated

by Brown and Strawley (64).

Schmidt (65) modified the ASTM procedure for metals and applied it to find the fracture toughness of limestone. He also conducted several direct pull tension tests which were used for compliance calibration. The crack length due to fatigue loading was estimated through the compliance calibration. Specimens were tested under three different orientations and statistically significant correlations between the fracture toughness and orientation were found. Schmidt and Huddle (66) investigated the effect of confining stresses on fracture toughness of Indiana limestone. It was shown that the fracture toughness of limestone increased with application of confining stresses. The specimens were tested as single edge notch specimens under direct pull tension. Schmidt and Lutz (13) had tested Westerly granite by the procedure described in (65). They showed that the thickness of the specimen had no effect on the fracture toughness. They also showed that fatigue pre-cracking was not necessary for testing rock fracture toughness. Ingraeffea and Schmidt (12) found that the fracture toughness of rock is dependent on the crack length. Hardy (67) and Hoagland, et al. (68) studied the inelastic behavior of rocks under tensile loads. In the absence of a viable plasticity theory for rocks, it was postulated that the inelastic behavior was due to microcracking. Schmidt (14) proposed a theory of the microcrack zone, similar to the plastic zone at the crack tip in metals, to model the fracture behavior of rocks. Henry, et al. (69) experimentally studied the crack propagation in calcite rocks. Through

experimental curves relating the crack propagation velocity and the stress intensity factors, it was possible to calculate the relations between stress and time to fracture and between fracture stress and deformation rate.

3.3 Mechanical Properties of Coal

This part of the literature survey will concentrate on the elastic properties of coal measured at room temperature. Although the underground coal may exist at considerably higher temperature than room temperature, the laboratory experiments were carried out at approximately 70°F ambient temperature.

The most extensive research was carried out by Ko and Gerstle (2) at the Colorado School of Mines. Here elastic properties of different coals were studied under controlled conditions. All the properties were measured under a compressive state of stress. It was found that although statistically coal might be regarded as an isotropic material, its Poisson's ratio, Young's modulus and modulus of rigidity do not satisfy the isotropic condition. Its bulk modulus does not even satisfy the transverse isotropy condition. Thus coal has to be considered as an orthotropic material. It was also observed that the compliance of coal does not depend on the magnitude of confining stress. The compressive strength of coal was found to be a strong function of confining pressure and is not dependent on orientations.

Evans and Pomeroy (70) have done extensive research on the mechanical properties of British coal. Evans (71) showed that the

tensile strength was significantly smaller than the compressive strength of coal. Cook, Ko and Gerstle (72) showed that the mechanical properties of British coals were significantly different from those of the U.S. coals. Thus this literature review will not include review of British coal properties within its scope.

Shoemaker (73) investigated the mechanical properties of Pittsburgh coal. His research concentrated mainly on the evaluation of the viscoelastic properties of Pittsburgh coal at elevated temperature. His data included values at 75°F. These values were within the comparable range of data published by Ko and Gerstle (2).

The compliance matrix of the Pittsburgh coal was obtained from the published work of Ko and Gerstle (2). These values were used to formulate the fracture mechanics model of coal (Chapter IV).

Almost all measurements of the mechanical properties of coal have been done using compressive loadings. Fracture, however, occurs in tension. Because of its lower tensile strength, measuring the tension moduli of coal is difficult. A measuring technique using pure bending of beams was developed. Barre de Saint-Venant (1797-1886) is believed to be the first one who actually examined the accuracy of the assumptions made in deriving the beam theory (74). He further studied the bending of beams of materials which do not follow Hooke's Law and have different moduli for tension than for compression. The relations between stresses and strains are of the form:

$$\sigma_t = A_1 \left[1 - \left(1 - \frac{y}{a_1}\right)^{m_1}\right] \text{ for tension} \qquad (3.1)$$

$$\sigma_c = A_2 \left[1 - \left(1 - \frac{y}{a_2}\right)^{m_2}\right] \quad \text{for compression} \tag{3.2}$$

where A_1, A_2, a_2, m_1 and m_2 are material constants and y is the absolute value of the distance to a point from the neutral axis. If the problem is limited to a rectangular beam of the cross-sectional area bh, then the neutral axis can be located by solving the following two equations:

$$y_{ts} + y_{bs} = h \tag{3.3}$$

$$\int_0^{y_{ts}} \sigma_t dy = \int_0^{y_{bs}} \sigma_c dy \tag{3.4}$$

He also calculated the moment of internal forces by using Equations 3.1 and 3.2 and then solved for the neutral axis position.

S. P. Timoshenko also investigated pure bending of a rectangular beam made from a material with different moduli of linear elasticity in tension and compression (75). He employed the strain energy approach to find the position of neutral axis:

$$y_{ts} = \frac{h\sqrt{E_t}}{\sqrt{E_t} + \sqrt{E_c}} \tag{3.5}$$

$$y_{bs} = \frac{h\sqrt{E_c}}{\sqrt{E_t} + \sqrt{E_c}} \tag{3.6}$$

and the bending moment:

$$M = \frac{4\ K\ I\ E_t E_c}{(\sqrt{E_t} + \sqrt{E_c})^2} \tag{3.7}$$

Attempts have also been made, especially in Russia, to derive the basic equations and relationships of the theory of elasticity, rather then elementary beam theory, for materials with different tensile and compressive strengths (76,77,78). To date these attempts have not been completely successful.

Even with the theories available, the tensile modulus of elasticity has been inferred from compressive tests for many design works due to the difficulties in performing tensile tests (79). The experimental measurements of elastic moduli of materials still follow the "standard methods" established by the ASTM (80,81) or the British Institute of Testing (82). The more convenient bending method is vastly used only in determining the "average" elastic moduli of timbers (83,84).

In 1969, L. Adler employed the "Transformed Section" concept (85) of Mechanics of Materials to determine the tensile modulus of elasticity of rock from one "standard" compression test and one flexural test (79). For a specimen of rectangular cross-sectional area bh made from a material of different linear moduli in tension then in compression, he derived an expression similar to Eq. (3.7).

$$E_r = \frac{4\ E_t E_c}{(\sqrt{E_t} + \sqrt{E_c})^2} \tag{3.8}$$

He further formulated the relation between E_t and E_c as:

$$E_t = n\ E_c \tag{3.9}$$

where n is determined by f(n):

$$f(n) = \frac{1}{(1 + \sqrt{1/n})^2} = \frac{3\ cL^3}{bh^3\ E_c}\ (\frac{P}{\delta}) \tag{3.10}$$

3.4 Hydraulic Fracturing Experiments

Hubert and Willis (86) ran experiments with gelatin specimens to simulate hydraulic fracturing and investigate some of the parameters affecting the hydraulic fracturing phenomenon. They suggested that most of the hydraulic fracturing (underground) should produce vertical cracks instead of radial horizontal cracks. They also suggested that the crack should propagate along the direction of minimum horizontal stress.† They performed their experiments with sand and other loosely packed materials. Their analysis predicting vertical cracks

---

†The stresses follow the engineering notation (tensile positive), which is reverse of common notation in the literature of hydrofracturing.

and direction were later verified in field and laboratory tests.

Haimson and Fairhurst (87) conducted experiments on cylindrical and cubical hydrostone specimens. They investigated the effect of fluid permeation on the critical or breakdown pressure (p_c) needed to produce fracture. The tests were conducted at a constant rate of pressurization. It was observed that the breakdown pressures were lower than those predicted for impermeable rocks and slightly higher than the predicted values for porous rocks ($\alpha = 0.82$). It was also observed that it was very likely to create a horizontal fracture at the bottom of the wellbore. They also found that the critical pressure decreased with the increase in the diameter of the wellbore.

Daneshy (88) conducted laboratory experiments on hydrostone, limestone and sandstone. He observed that the initial orientation of the crack is affected by the orientation of the borehole. But away from the borehole, the principle of least work would determine the orientation of the crack. In later work, Daneshy (89) further investigated inclined fractures and observed that shear failure was associated with the initiation and extension of all the inclined hydraulic fractures. These fractures, away from the borehole, also became perpendicular to the least compressive stress. The initiation and extension of axial fractures are caused by purely tensile failures of the borehole wall and surrounding formation.

Brechtel, et al. (90) ran laboratory tests on shale samples to determine the applicability of hydraulic fracturing to the method

of determination of in-situ stresses. They, however, did not account for the effect of fluid permeation (α) in their calculations. They concluded that the fracture did propagate along σ_{Hmin} and the shut-in pressure was an accurate estimate of the maximum principal stress (σ_{Hmax}) generally. Advani, et al. (91) studied the structural responses associated with hydraulic fracturing operations in reservoir rocks, through analytical and experimental simulations. Two and three dimensional finite element solutions were generated for the stress state around a crack tip and were compared with experimental results. The calculated fracture toughness from these experiments was within comparable range of results from other investigators. Ingraffea and Henze (92) used PMMA plates containing elliptical notch and subjected to biaxial loading at their edges. The cracks were initially inclined to the direction of the applied stresses. It was observed that the crack turned around as it propagated and aligned itself normal to the minimum compression load. Zodack, et al. (93) conducted laboratory hydraulic fracturing experiments to determine the possible dependence of breakdown pressure (p_c) upon the rate of pressurization and the influence of pre-existing cracks on the orientation of generated fractures. They found that the use of breakdown pressure rather than fracture initiation pressures might lead to an erroneous estimate of tectonic stresses.

At the Lawrence Livermore National Laboratory, Hanson, et al. are conducting extensive research on gas well stimulation processes through hydraulic fracturing. As mentioned earlier, this research

project closely followed the set-up developed at LLL (94). In several papers (95,96,97) the results of investigations have been reported. The current thrust in their research, as indicated by these papers, is to examine the effect of various field parameters (namely interfaces) on the geometry of fracture. All their tests were carried out in isotropic media or layered specimens made of isotropic materials.

Several hydrofracturing experiments have been carried out by Columbia Gas Company, Kentucky Gas Company, U.S. Bureau of Mines, etc. Capp, et al. (98,99) used hydrofracturing to create a burn path through a coalbed. These experiments were carried out by the U.S. Bureau of Mines. Elder, et al. used a vertical borehole (100) and hydraulic fracturing (101) for degasification of coalbeds. It was observed that the use of vertical boreholes coupled with hydraulic fracturing would provide for more rapid degasification and could provide a possible source of natural gas. These hydraulic fracture experiments were carried out with various degrees of success. Maza (102) evaluated gas flow reduction in nearby development mining and compared predicted and actual fracture behaviors in a Pittsburgh coal seam. A hydraulically created fracture was mined through and visual inspection indicated that the fracture width and length differed from predicted values by an order of magnitude.

3.5 Fluid Flow Problem in Hydraulic Fracturing

The volume of crack generated inside the pay zone is governed by the amount of pressurized fluid that is pumped in after accounting for the leak-off. Analytical study of this leak-off procedure is

dictated by the solution to a parabolic partial differential equation, with time dependent boundary conditions.

The fluid flow into the porous permeable material can be approximated by Darcy's law (103). This, when combined with the continuity equation, provides the necessary governing equation. This equation is similar to the familiar diffusion or heat conduction equation. Carslaw and Jaegar (104) solved the line drive model for a constant potential source using a summation procedure. For a constant potential point source the solution is available in closed form involving error-functions. There are no existing closed form solutions for non-isotropic material properties.

Howard and Fast (105) reported calculations performed by Carter for measuring the fracture volume. Different nomographs were presented for estimation of fracture area at different flow indices. Chang (106) used one dimensional model and Bernoulli's equation with assumed viscous friction losses to formulate the model of fluid flow in hydraulic fracturing. This model is approximately valid for flow in tight isotropic reservoirs.

Fluid flow inside the crack will govern the boundary condition along the crack for the fluid permeation into the medium. Quale and Levy (107) analyzed the problem of laminar flow in a porous tube. The flow was assumed to be steady and the fluid incompressible. Non-dimensional pressure ($2P/\rho U_0^2$) was calculated analytically and experimentally as a function of the radial Reynold's number (Re_r). In the case of uniform injection a method of similarity solution was

developed for the entire range of Re_r values.

The use of foam as a frac-fluid was developed because of its excellent viscosity and low sand-settling velocity. Blauer and Holocomb (108) discussed the bubble interference effects and reported the viscosity of foam as a function of the foam quality. In another paper (109), Blauer discussed the method of calculating the viscosity and friction loss from the consideration of the flow condition (laminar, turbulent, etc.), shear rate, etc. Ametov (110) investigated the filtration of aerated fluid in porous media and gave estimates of upper and lower bounds on the pressure distribution in the formation. This solution is non-linear in nature due to the pressure dependent properties of the aerated fluid. Blauer, et al. (111) further discussed foam properties and their effect on the stimulation procedure. Different expressions for effective viscosity and some empirical formulae for pressure drops were reported. Abbott, et al. (112) discussed the foam-frac in detail with a very good estimation of the cost involved. Foam-frac was shown to have higher production after several months than hydraulic stimulation and this is attributed to low fracture damage of the formation. Creaman (113) reported stimulation results for several Columbia gas wells. These stimulations were performed for comparison purposes. Sinclair (114) reviewed and discussed foam-frac. His calculations were based on the "fluid-loss-coefficient" reported by Howard and Fast (105). These calculations are valid for very low permeability and when the pressure drop along the crack is small enough to be ignored.

3.6 Analysis of Hydraulic Fracturing

In this part of the literature review, the main attention will be devoted to the problems which apply principles of mechanics to hydraulic fracturing. This will include both theoretical and numerical solutions for the state of stress in the media during hydraulic fracturing.

The first quantitative analysis of the two dimensional stress field around a wellbore, prior to fracture initiation, was done by Hubert and Willis (86). This was done by superposition of solutions for an infinite plane and a circular hole with far field stress. The magnitude of the pressure required to initiate the fracture could be computed from equations presented and it was pointed out that the pressure required to extend the fracture is slightly greater than the minimum principal stress.

Kehle (115) investigated the possibility of determination of in-situ stresses through hydraulic fracturing. He did not consider the effect of fluid permeation on the state of stress. Several field data were compared and tectonic stresses were estimated.

The effects of the tensile strength of the formation rock and of the pre-existing formation pore pressure on the pressure required to initiate and propagate a fracture from an underground wellbore were examined by Scheidegger (116).

Galle and Wilholt (117) made a three dimensional photoelastic study to determine the stresses around the wall and bottom of the wellbore due to fluid pressure within the wellbore and unequal

geostatic stresses. Their results are in good agreement with the stresses calculated by two-dimensional elastic theory.

The effect on the stresses around the wellbore of frac-fluid penetration into the porous formation was investigated analytically and experimentally by Fairhurst and Haimson (118,87).

Seth and Gray (119,120) formulated equations of elasticity for a transversely isotropic, axisymmetric, homogeneous, porous media exhibiting pore fluid pressure. Their investigation showed that porous and nonporous bodies with internal pressure had significantly different stress distributions and that anisotropic properties in the rock gave rise to a different stress distribution than did isotropic properties.

The orientation of fracture in an anisotropic material (coal) was investigated by Warren and Hayatdavoudi (121). In-situ stresses were calculated from field data of fracture initiation pressure and pore pressure. The in-situ horizontal stresses were calculated from the assumption of rigid containment.

The case of fracture initiation and propagation, for the problem where the wellbore direction does not coincide with one of the formation principal stresses, was analyzed by Daneshy (88,89). The equations from Hubert and Willis, Fairhurst and Haimson, and Kehle, along with a stress transformation technique were used to formulate the stress distribution equation around the wellbore. The angle between the formation principal stresses and wellbore direction was treated as an independent parameter. It was shown that the

orientation of the fracture changed as the fracture lengthened until it became perpendicular to the least compressive in-situ principal stress.

Daneshy, et al. (122) classified the treatment parameters for hydraulic fracturing into three categories: (a) controllable parameters, e.g., fluid density, fluid pressure, fluid viscosity, time, etc.; (b) partially controllable parameters such as fluid leak-off and injection ratio; and (c) uncontrollable parameters such as in-situ stresses, pore pressure, Young's modulus and Poisson's ratio of the rock, permeability of the formation, etc. Twenty-six examples of analytical models were studied to determine the effects of these parameters. It was seen that fluid viscosity had the most desirable effects on the fracture geometry by increasing the fracture width and decreasing the amount of leak-off. These 26 problems were analyzed in two dimensions with an assumed pressure distribution.

Two principal orientations of the fracture, horizontal and vertical, have been considered and analyzed under various assumptions. Horizontal cracks are generally assumed to be penny shaped and vertical cracks are assumed to be rectangular (105,123). Advani, et al. (124) studied the fracture propagation behavior from a fracture-mechanics viewpoint. Employing the stress intensity factor concept, the fracture was hypothesized to propagate by changing from a vertical elliptical crack to a penny shaped crack and consequently propagating with a semi-circular front. It was also shown that if the critical stress intensity ratio, $K_{Ic}^{(2)} / K_{Ic}^{(1)}$, between the

barrier rock layer and the payzone layer is greater than 1.57, the fracture is confined in the payzone. Simonson, et al. (125) investigated the fracture containment as affected by different material properties between payzone and barrier zone, in-situ stresses and hydrostatic pressure gradients. A two dimensional analysis showed that the hydraulic fractures in a payzone located between two adjacent barrier layers would tend to be confined provided that the barrier layers were stiffer than the payzone and that the in-situ stress was greater in the barrier layer.

Perkins and Kern (126) formulated an equation for the fracture width as a function of rock elasticity, injection rate, fracturing fluid properties and fracture height. This expression is independent of injection pressure. Geertsma and de Klerk (127) considered the crack in a horizontal section and, assuming a parabolic fluid distribution, formulated an expression for crack width. Generally, crack height (vertical) is smaller than the crack length (horizontal), and thus crack displacement should be controlled by its vertical section. Advani, et al. (128) considered this factor and modified the expression formulated in (127). From a standpoint of fracture mechanics, for the plane strain problem, Advani, et al. (129) formulated the fracture width for an elliptic crack.

Daneshy (130,131,132) studied the effects of material properties and layering on the propagation of cracks. A term, similar to the stress intensity factor under plane strain conditions, was defined as the fracturability index of the rock. A smaller value for the

fracturability index ($E/[1-\mu^2]$) indicated that the fracturing would be easier. It was also shown experimentally that fracture containment within a particular zone was extremely difficult. Experiments (132) also showed that the elliptic crack induced from a line source tended to become penny shaped.

Shuck and Advani (133) investigated the stress field induced by hydraulic fracturing in a non-permeable media. Two dimensional and three dimensional elasticity theory models were formulated and solved for the static field and local stress distribution during a fracture extension phase. This study, with emphasis placed upon stress analysis, provides a better understanding of the mechanism of the hydraulic fracturing process.

Ruina (134) investigated the coupled deformation-diffusion effects on the hydraulic fracturing process. Hydraulic fracture of a saturated porous rock formation is discussed taking into account the full coupling between matrix deformation and ambient pore fluid diffusion. General results were found analytically and some detailed results were obtained numerically.

Gangarao, et al. (135) used the finite element method to evaluate the stress field induced by hydraulic fracturing. In addition, analytical and experimental simulations of the structural response have been studied (124,136,137) in terms of fracture configuration, fracture dimension, and critical fluid pressure.

Advani (138) used the finite element method for the width equation and provided a framework for evaluation of fracture dimensions

and associated responses. The roles of multilayering, joint interaction and branch cracks along with comparison with other work and their applications were discussed.

Cleary (139) discussed the effect of anisotropy on the stress concentration near the borehole. Effects of fluid penetration and the in-situ stresses on the fracture initiation and propagation were discussed. Several recommendations were made to improve the hydrofrac operations.

IV. RESULTS

Four basic types of experiments were conducted; three point bending fracture toughness tests, direct pull tensile strength tests, elastic bending tests and hydraulic fracturing experiments. The experimental procedures and equipment used, specimen collection and preparation techniques, and computer programs developed are described in detail in the appendices. All the results of the experiments are also tabulated in the appendices. Because coal has directions of natural weakness, all test results must include a description of the specimen orientation. The following convention (Figure 4.0.1) was adapted: the direction of the principal material axes 1, 2 and 3 are defined as the normals to the major (face) cleat, minor (butt) cleat and bedding planes, respectively.

The Pittsburgh coal seam was selected for most of the experimental work because of its commercial importance, the large amount of methane in the seam, the availability of information about this coal and the accessibility of specimens in northern West Virginia. Redstone and Waynesburg coals were also tested to provide comparisons. Because these coals are strip mined they were often available in the larger pieces needed for specimen preparation.

The three point bending fracture toughness tests used in Tasks 1, 2, 6 and 7 involved loading a notch beam to initiate a crack at the notch tip. The load needed to create the crack is used to compute fracture toughness. This procedure is based on the ASTM Standard E399 as modified (13,14,65) for testing of rocks. The basic apparatus (Figure 4.0.2) involves supporting the ends of the beam and loading

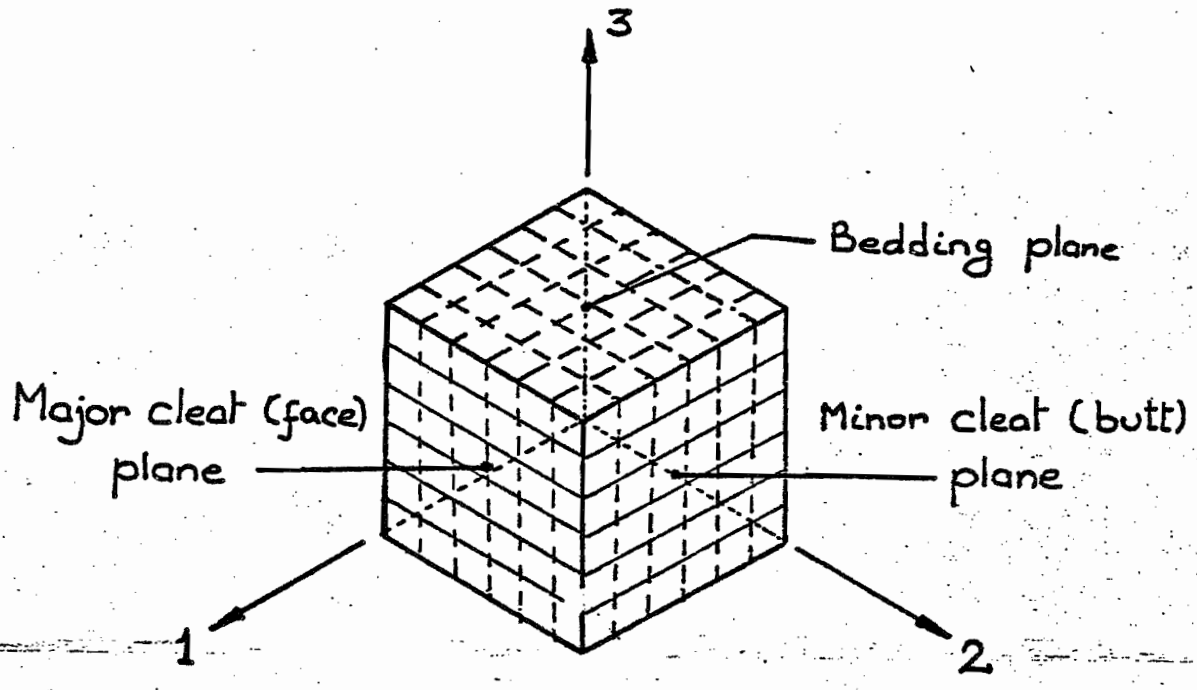

Figure 4.0.1 Relation of axes used in research to the natural planes of the coal seam.

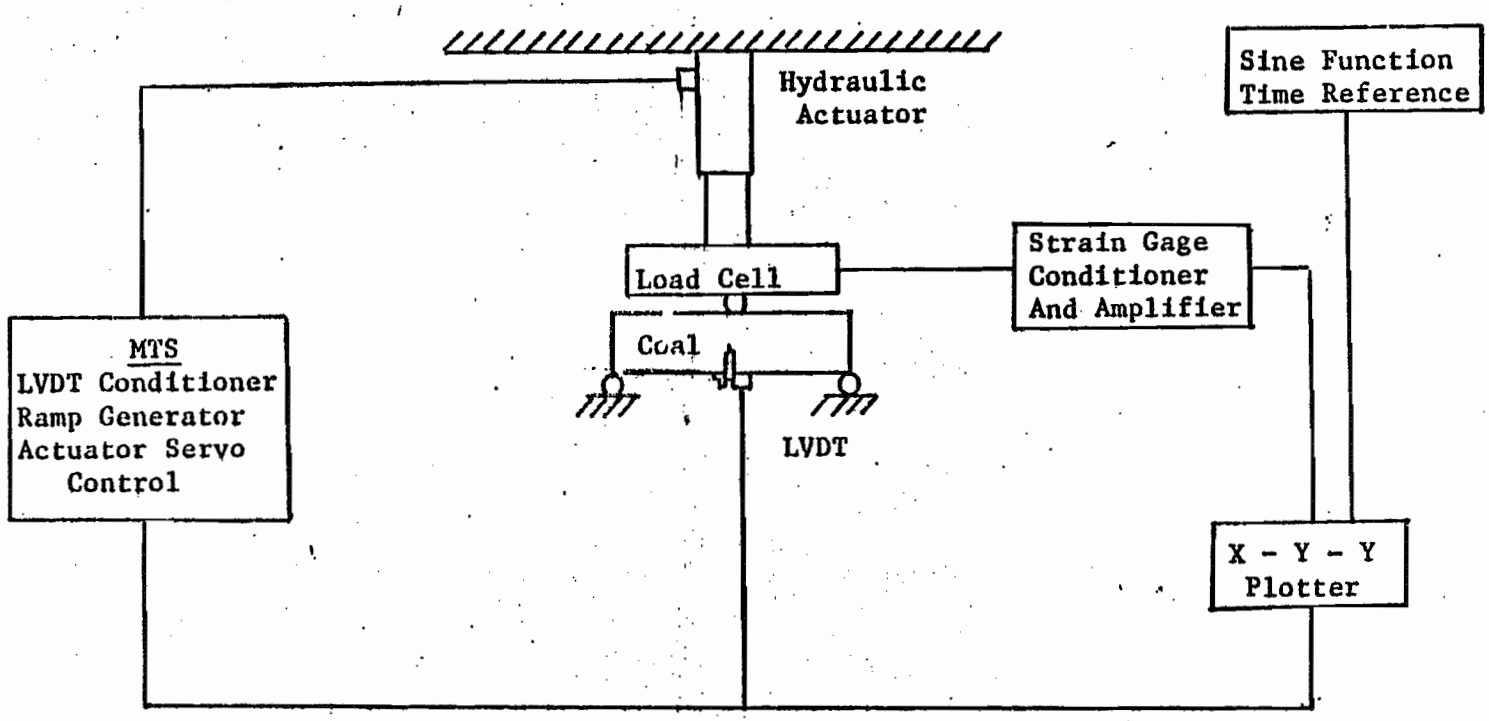

Figure 4.0.2 Schematic drawing of the experimental apparatus used for fracture toughness tests.

the center (over the notch) by an MTS servoram. An LVDT measures notch opening which is used as a feedback control signal to the MTS system to create a controlled deformation loading and eliminate dynamic fracture propagation. Detailed descriptions of the apparatus and testing procedure are given in Appendices 1, and 2.

The direct pull tensile strength tests for Task 5 are also a modification of an ASTM standard (81), Standard D-2936-71, for testing rock core specimens. The tests differed from the standard in that specimens with non-circular cross sections were used. The tests measured ultimate tensile strength. The details of the equipment and procedure are contained in Appendices 1, and 2.

The elastic bending tests used to create data for Task 5 were developed independently during the research. They were used to determine compressive and tensile elastic moduli of coal. The details are given in Appendices 1, and 2.

As indicated earlier, the hydraulic fracturing experiments for Tasks 3 and 4 were designed after the procedure and designs developed at the Lawrence Livermore Laboratory (94). The basic experimental apparatus involves a cylinder-plunger system which drives the fluid through a stainless steel tube into a cubic specimen (Fig. 4.0.3). The plunger was driven by a MTS servoram with a servac feedback control system. The cubic specimen was placed in a load chamber and its sides were pressurized through fluid filled flat jacks to simulate the maximum and minimum horizontal stresses and the overburden stress. A hole was drilled at the center of the top face. The hole extended to the lower one-third of the specimen height. Fluid from the cylinder-plunger system was

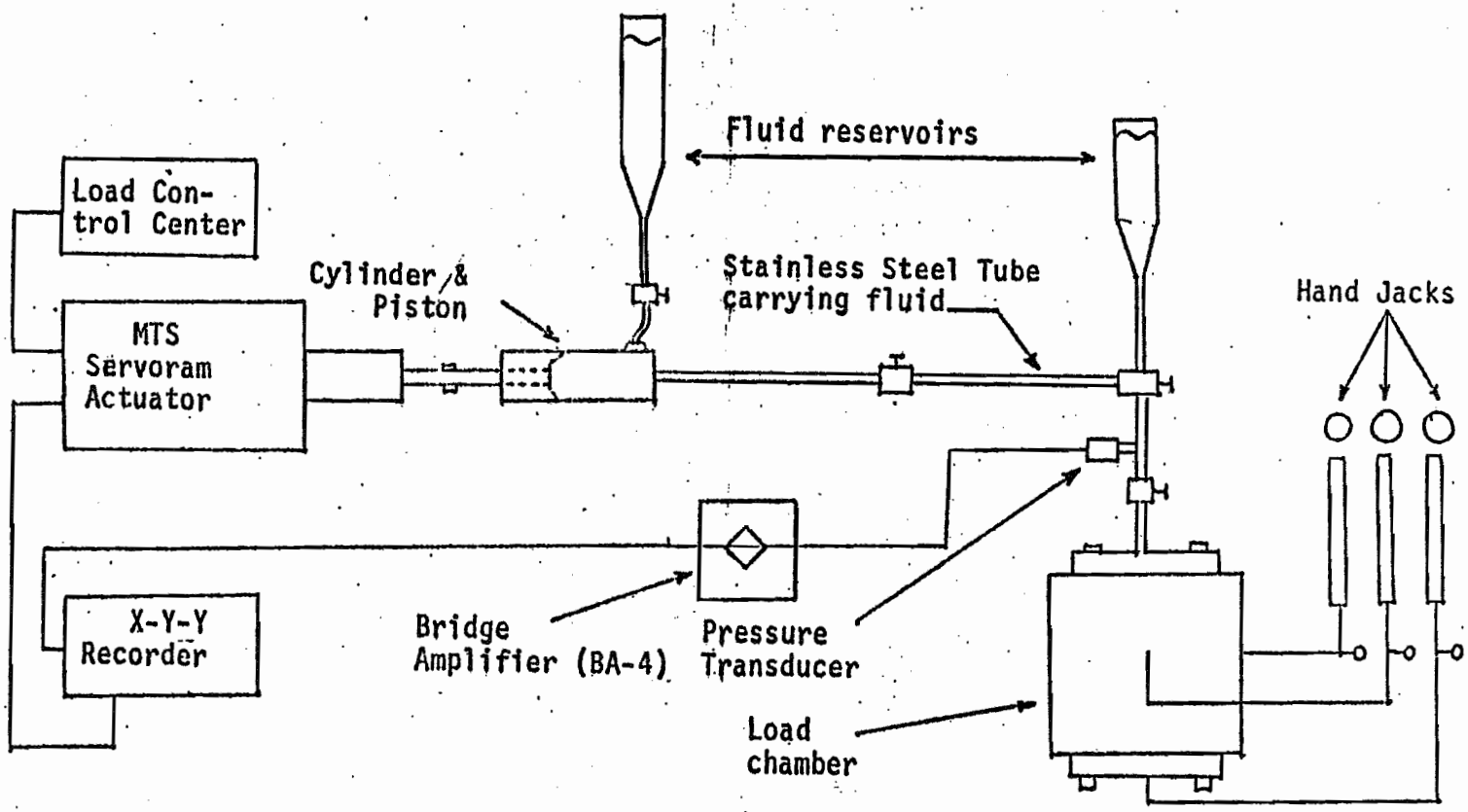

Figure 4.0.3 Schematic Drawing of Experimental Set-up for Hydraulic Fracture Experiment.

injected into this simulated borehole. Detailed descriptions of the apparatus and testing procedure are given in Appendix 1, and 2.

Zodack, et al. (93) have shown that, for sedimentary rocks, fluid flow rate controlled experiments produced more consistent results than fluid pressure controlled experiments. Under field conditions, hydraulic fracturing is carried out with constant fluid flow rates. Thus it was decided to conduct the experiments with controlled fluid injection rates.

The following values of the parameters will be defined as the "standard values".

(i) Fluid flow rate: 4.712×10^{-3} cu.in/sec

This volume flow rate was produced by a .001 H_z frequency saw tooth wave control signal for the hydraulic servoram (MTS). This was the minimum frequency available in the feedback system. This velocity was chosen such that the Reynold's number of flow through the crack opening was of the same order of magnitude as under the field condition. Also, this fluid flow rate minimized any dynamic effect in the experiments.

(ii) Orientation of the specimen: The bedding plane was kept perpendicular to the overburden stress, the face plane perpendicular to the minimum horizontal stress and butt plane perpendicular to the maixmum horizontal stress. This condition simulates the most frequently encountered orientation of coal seams under stable field conditions. The induced fractures ran parallel to the face cleat.

(iii) In-situ stresses: 400 psi - minimum horizontal
600 psi - maximum horizontal
1200 psi - overburden

These standard horizontal stresses were chosen from field data of actual hydrofracturing done in nearby Washington County, Pennsylvania. The overburden stress chosen was the maximum pressure attainable through the flat jacks.

(iv) Fluid viscosity: 19 cps (hydraulic oil)

The standard fluid was chosen to be hydraulic oil because of its availability coupled with the consistency of its properties.

The experimental results for the individual tasks follow.

4.1 Task 1 - A total of 73 tests were conducted of which 36 yielded useful results to determine the fracture toughness (critical stress intensity factor) of coal. Apparatus specimen preparation, and testing procedure are described in Appendices 1, 2 and 3 respectively. The tests were conducted with the specimen sides, the fracture, the loading and the stresses orthogonal to the natural axes [1, 2 and 3].

For Pittsburgh coal the three orientations shown in Figure 4.1.1 were selected to have either the stress or the crack propagation normal to the bedding plane. The tests on the Redstone and Waynesburg coals involved only one orientation each. Specimen preparation was attempted on some additional orientations but was usually unsuccessful because cleating made cutting 6 inch long specimens nearly impossible. Two specimens of Pittsburgh coal were successfully cut in Orientation 21; one specimen was successfully tested and had K_{Ic} equal to 21.2 psi-$\sqrt{in.}$. This sample size of one is not large enough to make any statement about the actual value of K_{Ic}.

The test results for the different orientations are listed in Table 4.1.1. For all orientations, the sample size was large enough to

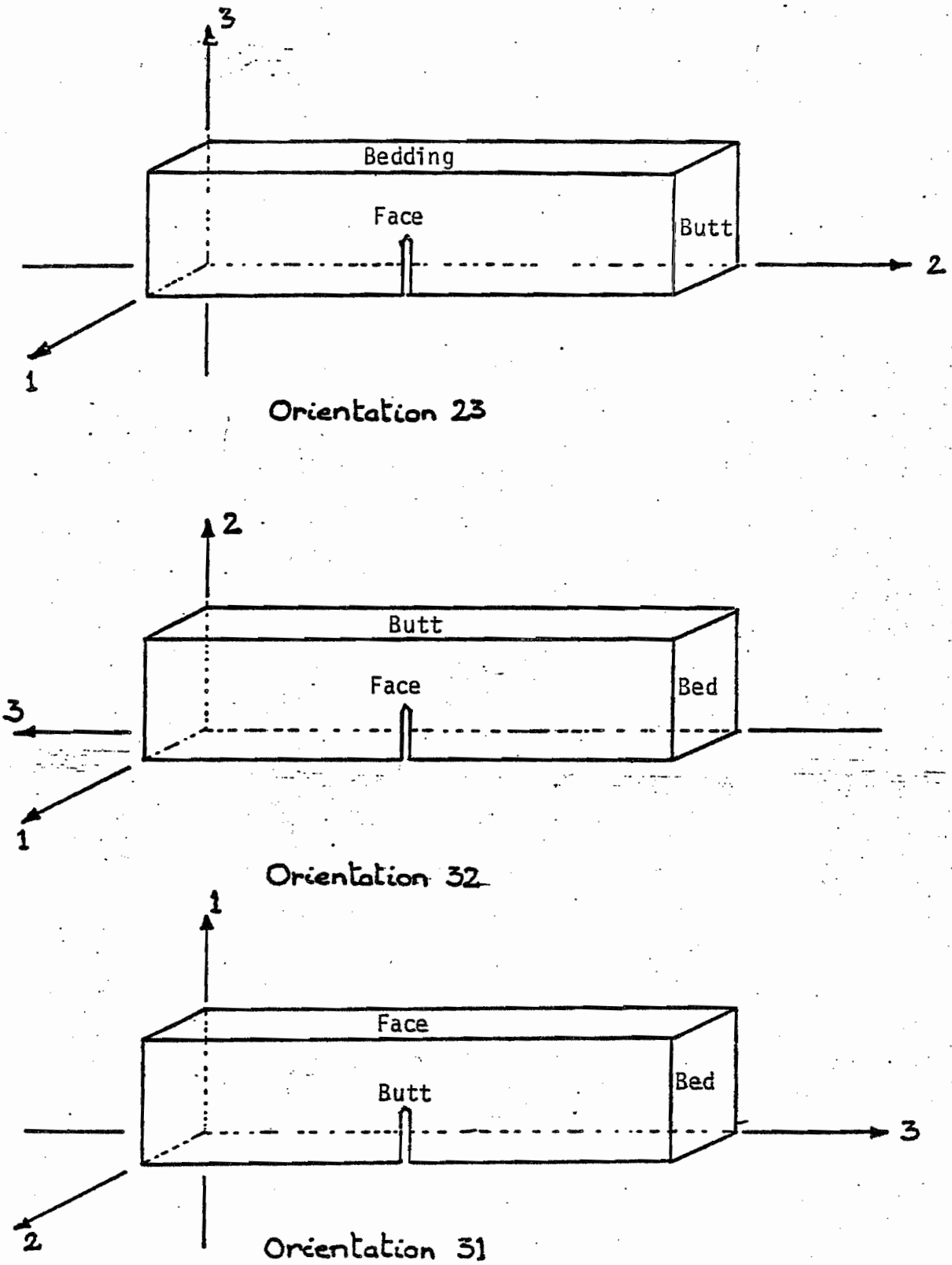

Figure 4.1.1 The three orientations of Pittsburgh Coal which were tested for fracture toughness

Coal	Orientation	Sample Size	Mean $K_{Ic} \pm$ S.D. (psi-√in)	(kN/m$^{-3/2}$)
Pittsburgh	23	16	56.48±22.95	62.78±25.31
	32	22	41.23±14.30	45.46±15.77
	31	6	42.72±22.88	47.11±25.23
	[31 & 32]	28	41.52±15.50	45.89±17.09
Redstone (Low K_{Ic})	32	8	22.14±6.70	24.41±7.39
(High K_{Ic})	32	4	94.28±28.05	103.97±30.93
(Combined)	32	12	47.19±38.79	51.34±43.12
Waynesburg	32	5	99.65±48.80	109.87±53.80

Table 4.1.1 Critical Stress Intensity Factors for Three Coals Based on 3-Point Bend Tests.

have statistically valid results. In some cases, additional results from tests performed previous to the contract were added to enlarge the sample size. The results of every test are listed in Appendix 4. For Pittsburgh coal the fracture toughnesses for orientations 32 and 31 are nearly identical at 41.6 psi$\sqrt{in}$. This result was expected because these orientations have fractures parallel to the bedding planes. Statistical analyses (t-tests at the 0.01 significance level) indicate no significant difference between these results; therefore, they are combined in Table 4.1.1 and in all modeling work.

There is a statistically significant difference between the fracture toughness, 56.5 psi$\sqrt{in}$, for orientation 23 and for orientations 32 and 31. The critical stress intensity factor is approximately one third larger for fracturing across the bedding planes than for along them. The difference between vertical and horizontal fracturing of a coal seam plays a key role in the modeling work described in Section 3.5. The fracture toughness results for the other coals, 47.2 for Redstone and 99.6 for Waynesburg are different but of the same order of magnitude as the ones for Pittsburgh coal.

The fracture toughness test results for Redstone coal appeared to be bimodal in distribution and are listed as two groups; high K_{Ic} and low K_{Ic}. In an attempt to correlate this difference with some other characteristic of the specimens, samples were sent to the W.V.U. Coal Research Bureau for chemical analyses and grindability tests. The results of these tests show no obvious correlations between fracture toughness and these other properties. However, there is not enough data to state conclusively that there are no correlations.

The mechanical properties of coal are known to be visco-elastic (73) or rate dependent under certain conditions. Therefore, the effects of loading rate on fracture toughness were investigated by varying the notch opening rate (NOR) for the tests on orientation 31. Three rates were used; 9.1×10^{-4} in/min, 18.9×10^{-4} in/min and 110.6×10^{-4} in/min. These rates are listed on Table A.4.2. Figure 4.1.3 shows the mean critical stress intensity factors for each group plotted against loading rate. Statistical tests indicate no significant differences in fracture toughness for the three loading rates.

4.2 Task 2 - In this task, the tests were intended to not only measure fracture toughness but also to determine if fractures would follow the direction dictated by stresses (vertical) or follow the bedding and/or cleating. A test was a success as long as the fracture started at the notch tip; fifty [50] tests were performed, forty-four [44] proved useful. The results of each of these tests are listed in Table A.4.9. Specimens were cut with the angle between the bedding plane and the notch, Figure 4.2.1, being 75, 60, 45, 30 or 15°. This represents rotating the specimen orientation about axis 1. The 15° degree increment was selected as it is slightly larger than the ± 10° band defined as acceptable in the fracture toughness standard (63). Specimen cutting at orientations produced by rotations about axes 2 and 3 was attempted but was unsuccessful because of the size of the coal blocks and fractures during cutting.

The results are summarized in Table 4.2.1 and Figure 4.2.2. The results indicate that fractures cannot be expected to cross the bedding planes unless the angle between the fracture and the bedding approaches seventy-five degrees. For angles less than this, the probability (in

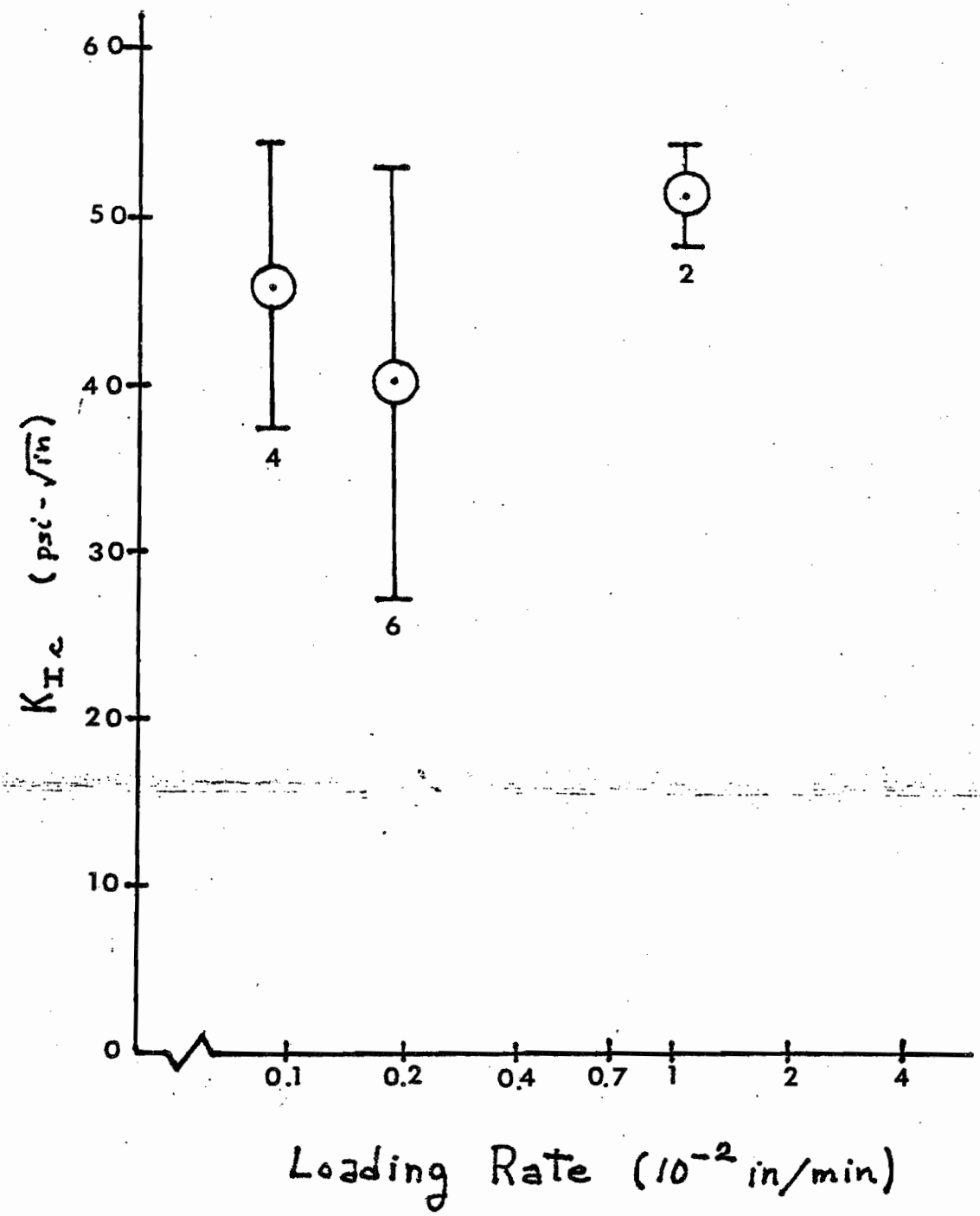

Figure 4.1.3 Variation in Mean Fracture Toughness Results with Loading Rate. The numbers under each point represent the number of tests, the bars show ± one standard deviation.

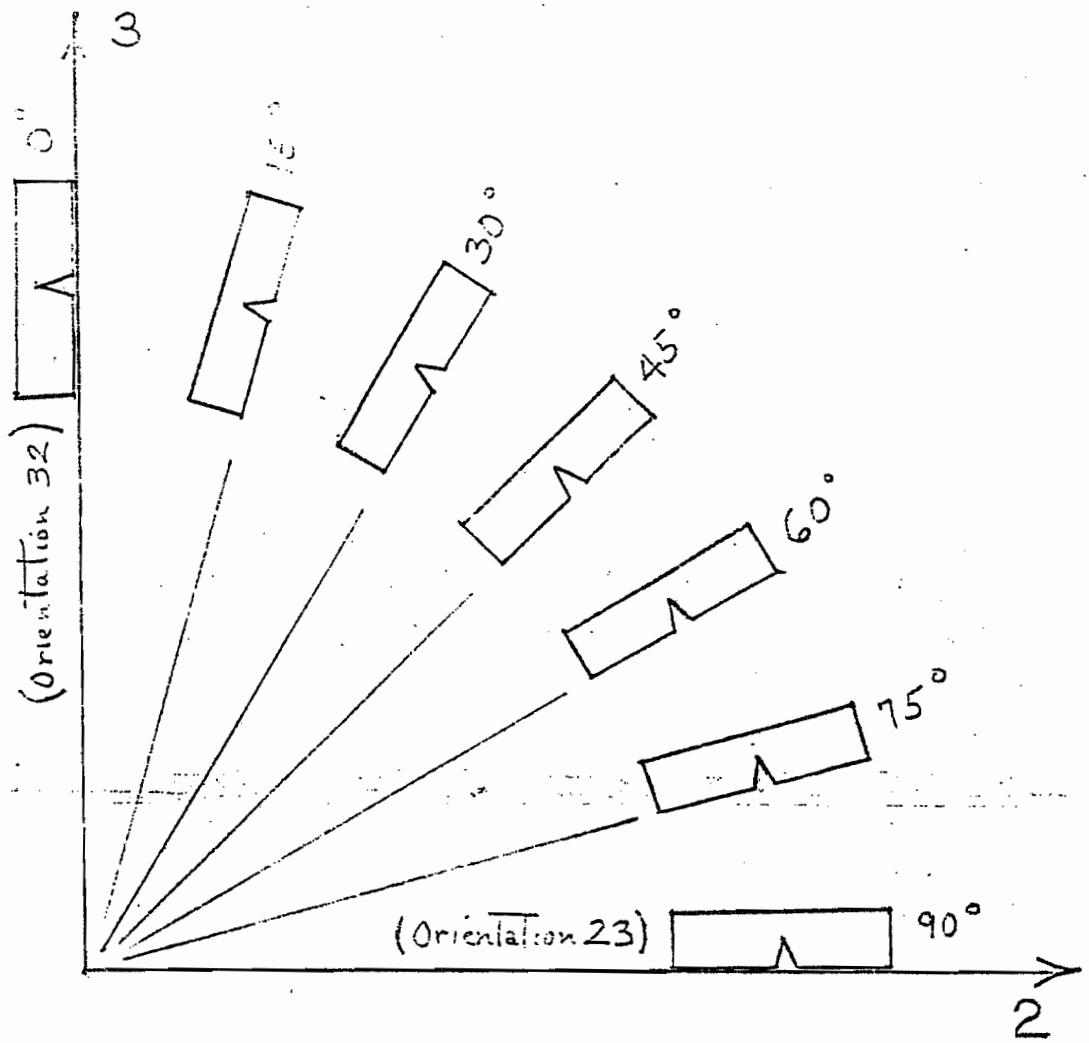

Figure 4.2.1 Specimen Orientations (75° - 15°) tested in Task 2. All orientations are defined by rotating specimen about the 1 axis. Orientations 90° and 0° were tested in Task 1 as 23 and 32 respectively.

θ (deg)	Number of tests	Fracture Pattern A No.	%	K_{Ic} (psi - √in)
	-	-	-	
90°	-	-	-	56 .48±22.95
75°	8	5	62	38.46±25.80
60°	5	1	20	18.72
45°	17	3	18	74.14±46.53
30°	6	1	17	41.63±14.30
15°	8	1	12	27.8
0°	-	-	-	41.23±
Total	44			

Table 4.2.1 Summary of Test Results with Bedding Planes Oblique to the Fracture. Ninety degrees is orientation 23; zero degrees is orientation 32. Except at 0° and 90°, there are not enough values of K_{Ic} to be statistically meaningful.

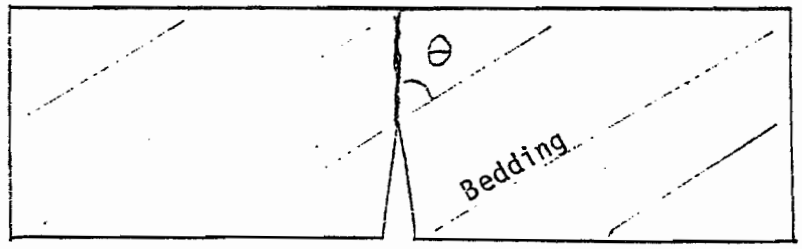

(A) (Vertical)

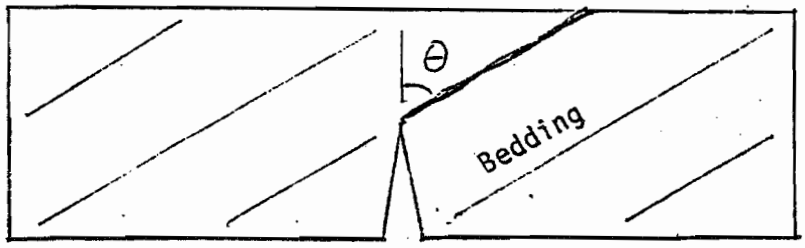

(B) (Along Bedding)

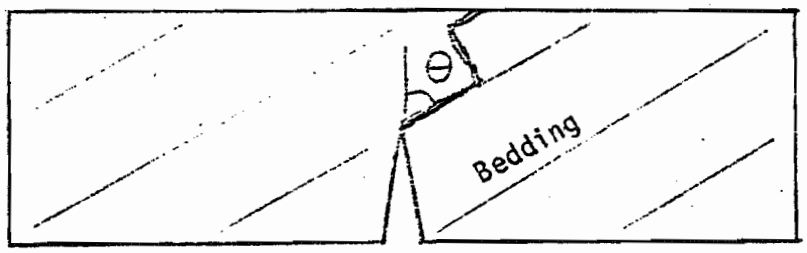

(C) (Along Bedding and Cleat)

Figure 4.2.2 The Three Fracture Patterns Seen in Oblique Testing. Fractures nearly always propagated initially along bedding rather than along cleat.

the absence of confining stresses) of a fracture crossing the bedding is 20% at best (6 specimens out of 32 tested). Not enough fracture toughness values were obtained for each angle less than seventy-five degrees to attach any statistical significance to the numbers or differences between them.

The results for 45° indicate the relative weaknesses of bedding and cleating. The two planes are at equal angles to the notch yet all of the fractures started to propagate along the bedding. Some fractures did change directions and ended up being along both bedding and cleating (pattern C in Figure 4.2.2); the significance of these directions changes cannot be determined because of the extremely complex stress state at the tip of a crack propagating obliquely to the bending stress field. Most likely there are some cleats weaker than the bedding planes but there are so few compared to the layers of bedding that all propagating fractures were found to be deflected by a bedding plane before they crossed one of these weak cleats.

4.3 Task 3 - A total of forty-five [45] hydraulic fracture simulations were attempted; thirty-eight [38] of which yielded useful results. Appendix 5 contains lists of all the results. The goals of this task were to evaluate the effects of loading rate (fluid flow rate) and specimen orientations.

The bottleneck of the experimental program was the repair or replacement of ruptured flat jacks. Thus the first set of experiments were conducted to observe the effect of variation of the flow rate, as these experiments could be carried out with small confining stresses which minimized the likelihood of flat jack ruptures.

Three values of fluid flow rate were chosen:

(i) 4.712×10^{-3} cu.in/sec (0.006 in/sec ram speed)

(ii) 22.78×10^{-3} cu.in/sec (0.029 in/sec ram speed)

(iii) 45.55×10^{-3} cu.in/sec (0.058 in/sec ram speed)

The ram speed of 0.006 in/sec was estimated to simulate the actual fluid dissipation (leak-off) velocity observed in field tests. The maximum fluid flow rate (.058 in/sec ram speed) was limited by the dynamic response of the recorders. The intermediate flow rate was selected as half of the maximum rate.

The effect of fluid flow rate is coupled with the effect of fluid penetration into the coal. The critical pressure of fracture initiation is dependent on the fluid penetration parameter (87). It has been shown that for an isotropic and porous material and a penetration fluid:

$$p_c = \frac{\sigma_t - 3\sigma_{22} + \sigma_{11}}{2 - \alpha \left(\frac{1-2\nu}{1-\nu} \right)} \tag{4.1}$$

where

p_c = critical pressure

σ_{22} = maximum effective horizontal stress

σ_{11} = minimum effective horizontal stress

σ_t = ultimate tensile strength

$\alpha = 1 - \frac{C_r}{C_b}$

C_r = compressibility of the rock

C_b = bulk compressibility of the rock